Co-Heating method for thermal performance evaluation of closed refrigerated display cabinets

International Journal of Refrigeration 121 (2021) 51–60

Contents lists available at ScienceDirect

International Journal of Refrigeration

journal homepage: www.elsevier.com/locate/ijrefrig

Co-Heating method for thermal performance evaluation of closed refrigerated display cabinets

Tommie Månsson*, Angela Sasic Kalagasidis, York Ostermeyer

Building Technology, Architecture and Civil Engineering, Chalmers University of Technology, Gothenburg, Sweden

ARTICLE INFO

Article history:
Received 14 April 2020
Revised 8 October 2020
Accepted 9 October 2020
Available online 13 October 2020

Keywords:
Refrigerated display cabinet
Thermal performance
Experiment
Condensate
Co-Heating

ABSTRACT

In this study, an application of the adapted Co-Heating methodology for thermal performance evaluation of closed refrigerated display cabinets (RDCs) has been presented. A novel test series comprising three experiments has been developed and demonstrated on a commercial RDC with four doors to evaluate the envelope heat transfer coefficient, thermal inertia, infiltration at idle state and dynamic infiltration caused by door operations. The latter two experiments were conducted in parallel with the condensate collection method for validation of the results for infiltration. It was concluded with good (<10%) conformance between the methods that the infiltration at idle state for the tested RDC is approximately 0.022 kg/s and that one 15 s door opening causes approximately 0.94 kg of ambient indoor air to infiltrate. Additionally, the time, equipment and associated costs for running the tests were compared, and it was concluded that the adapted Co-Heating methodology could substitute the condensate collection method for the evaluation of infiltration while providing additional results on the thermal performance.

Méthode de co-chauffage pour l'évaluation des performances thermiques des meubles frigorifiques de vente fermés

Mots clés: Meuble frigorifique de vente; Performance thermique; Expérimentation; Condensat; Co-chauffage

1. Introduction

Global initiatives to reduce the climate impact of electrical energy generation are leading to an increased share of renewable energy sources in the energy mix. However, the electrical power generated from renewable energy sources such as solar, wind and wave energies cannot be adapted to the electrical demand in the same flexible way as gas, coal and hydro. Therefore, there is a need to add energy storage capacity in a grid with a larger share of these non-dispatchable renewable sources (Farhangi, 2010).

The purpose of the added energy storage capacity in the grid is to bridge the time-shift between the supply of electrical power from the non-dispatchable sources to the energy demand of the end-users. Within the storage units, the electrical energy is commonly stored as a potential that later can be regenerated into electricity such as electrochemical potential in batteries or gravitational potential energy in pumped hydropower plants. Consequently, to provide the needed energy storage capacity, investments in storage infrastructures are required.

Alternatively, to reduce the need for intermediate energy storage, the end-users could adapt their electrical energy demand to the available supply, i.e. demand-side response (Albayati et al., 2020; Khan et al., 2018). For some processes with large inertia, the electrical energy demand could be increased or reduced for a period of time without noticeable consequences for the end-user. One such example is the energy intense refrigeration systems of supermarkets that potentially could be used for demand-side response purposes. This potential has previously been concluded and discussed in Albayati et al. (2020), Funder (2015), Hovgaard et al. (2011), Månsson and Ostermeyer (2019), Månsson and Ostermeyer (2013),

* Corresponding author.
E-mail address: tommie.mansson@chalmers.se (T. Månsson).

https://doi.org/10.1016/j.ijrefrig.2020.10.011

Nomenclature

C	Heat capacity J/kg
ξ	Correction factor –
c_p	Specific heat capacity J/kgK
K	Heat transfer coefficient W/K
m	Mass kg
$\dot{m}$	Mass flow rate kg/s
p	Pressure Pa
$\dot{Q}$	Heat flux rate W
R	Gas constant J/kgK
ρ	Density kg/m^3
t	Time s
τ	Temperature K
T	Temperature °C
X	Moisture ratio g/g_D

Subscripts

Amb	Ambient
Cond	Condensate
Corr	Corrected
CO,i	Condensate collection method, Step *i*
COH,i	Co-Heating method, Step *i*
D	Dry air
Env	Envelope
Exf	Ex-filtration
i	General index
In	Indoor
Inf	Infiltration
Int	Internal
Opening	Door opening
RDC	Refrigerated display cabinet
T	Total
W	Water (or water vapour)
Ws	Saturated water

and Pedersen et al. (2014). The thermal inertia of the refrigerated food and infrastructure connected to the refrigeration system allows the system to shift the time of energy use for periods of time in the magnitude of minutes. The time-shift is relatively short because any violation of temperatures outside the allowed range for refrigerated goods would be devastating as the value of the goods far outweighs the cost of energy. Therefore, it would be required to have a highly detailed understanding of the thermal loads affecting the temperatures of the refrigerated goods in the supermarket to implement control strategies that allow the electrical grid to utilise this resource.

An example of the thermal response to a cooling and heating cycle of a refrigerated display cabinet (RDC) can be found in Månsson and Ostermeyer (2019), which is also presented in Fig. 1. Here the temperature is reduced as the refrigeration system extracts heat from the RDC. Once the temperature has reached a lower limit (6.3 °C), the heat extraction process ends. Subsequently, the internal and ambient thermal loads will increase the temperature in the RDC until the upper limit (7.7 °C), and then, the heat extraction process starts again. The frequency and duration of the processes are depending on the intensity of the thermal loads and the heat capacity of the RDC. The larger the heat capacity, the slower the processes. Conversely, an increased thermal load would cause the temperature to increase faster and thereby shorten the duration of the period without any heat extraction demand.

The heat gains of the RDC comprise a baseline load by infiltration through gaps and conduction through the envelope, which are respectively proportional to the enthalpy and temperature difference between the ambient air and the air inside the RDC.

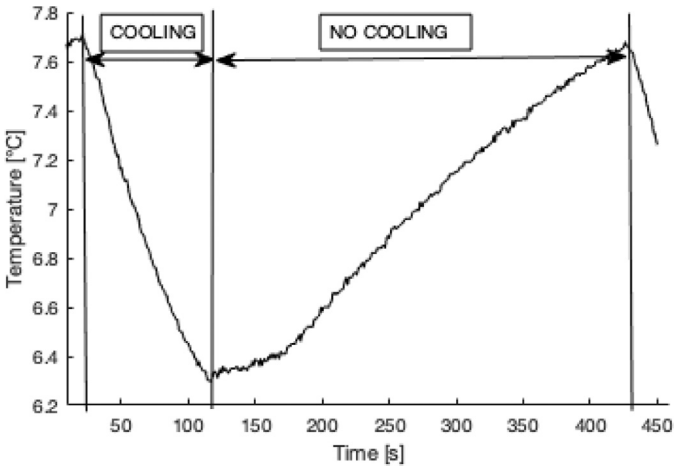

Fig. 1. Temperature variations in an RDC from Månsson and Ostermeyer (2019). When refrigeration is active, the temperature decreases from 7.7°C to 6.3°C within approximately 100 s. The temperature is then increasing back to the upper limit of 7.7°C for 300 s before the refrigeration cycle begins again.

Additionally, internal heat gains from lights and fans inside the RDC are constant during the opening hours of the supermarket, and normally the lighting is then reduced while the supermarket is closed. Furthermore, the operation of the doors of the RDC constitutes the only short-term variable thermal load for the RDC (Månsson, 2016). The door opening frequency, duration and angle vary significantly in time and between different RDCs in a supermarket (Månsson et al., 2019). Hence, as the thermal load varies in time and between individual RDCs, so does the heat extraction demand of the individual RDCs.

If supermarket refrigeration systems are to be utilised for demand-side response, the available buffering capacity should be monitored, i.e. when and for what duration the refrigeration system can be turned off or, alternatively, ran on reduced or increased power without violating the temperature limits of the goods stored in the RDCs. As an indicative measurement for the duration of these cooling and heating processes, the time constant, t_c, for the system can be used. $t_c = C_{RDC}/K_{RDC}$ describes the time it takes for a relative step-wise temperature change in a linear thermal system. Larger values of t_c indicate a system with larger thermal inertia and vice versa. Based on experience from earlier experiments, t_c for an RDC with doors is approximately 2 h at idle state and 1 h when the doors are operated at peak hours, i.e. the demand response potential is affected significantly by the door operations. It is, however, important to notice that the time constant can only be used as an indicative measurement as parts of the loads are latent.

To gain adequate insights on the thermal performance and, thereby, the demand response potential of an RDC the influencing variables for heat gains such as the heat transfer coefficient of envelope (K_{Env}), infiltration rate of air through gaps ($\dot{m}_{Inf}$) and by door openings ($m_{Opening}$), as well as the heat capacity of the RDC and its content (C_i), should be quantified.

In Faramarzi (1999) the author presented a study where the thermal load components of an open RDC were defined and estimated by heat transfer calculations and experimental experience. Based on this study, infiltration was found to be the most significant contributor for thermal loads for the RDC (73%). Additionally, the author concluded that infiltration is the most challenging aspect to evaluate.

In a follow-up study (Faramarzi et al., 2002), the authors applied a method where the condensation water was collected to compare the infiltration rate to an RDC with and without doors. When doors were installed, a reduction of 68% in total heat

extraction demand was determined. Consequently, the remaining thermal loads become significantly more important. However, infiltration remained the single most influencing factor, representing 50.6% of the total thermal load after doors were installed.

For the evaluation of infiltration, an alternative to the Condensation collection method is the Enthalpy method presented in Navaz et al. (2005). Here, the authors presented a method where the infiltrating air of an open RDC can be evaluated by measuring the mass flow rate of the supply air of the RDC and the enthalpies or temperatures of the spilling air from the RDC, ambient air as well as the discharge and return air of the RDC.

Later, in Amin et al. (2009), a tracer gas method for the evaluation of infiltration based on the concentration of a tracer gas at certain points in and around the RDC was presented. Besides the gas concentration in the discharge air, return air and ambient air, the mass flow rate of the discharge air must also be known to evaluate the infiltration rate with this method.

The methods mentioned above only evaluate the infiltration, and the Enthalpy method is limited to open RDCs only. The Tracer gas method requires significant investments to accurately distribute and measure the tracer gas concentration in the RDC, whereas the Condensation collection requires only an elevated moisture content of ambient air. To the best of our knowledge, there is no existing experimental methodology that can be used to evaluate both the thermal performance variables and the infiltration of an RDC simultaneously.

As an alternative to experimental work, in Orlandi et al. (2013) the authors presented a study where the thermal load caused by operation of sliding versus hinged doors was compared based on the results of dynamic CFD simulations. The relation between thermal loads from individual components was also evaluated and presented for the two door types, by including both the scenario with and without customer interactions. Based on the results, the conduction through the envelope of the RDC with two hinged doors contributes to 70% of the overall thermal loads during nighttime when the RDC is idle. During daytime, the contribution decreases to 44% as the influence of infiltration through door openings increases significantly. Regardless of time, the thermal loads caused by transmission through the envelope are of magnitudes that demand careful evaluation. In the conclusions, the authors emphasise the possibilities to separate influencing factors and investigate isolated details of an RDC in the computer models. However, significant efforts must be made to find data on material properties and to geometrically depict the RDC with all internal and external details that might affect the results.

In the search for alternative, more comprehensive experimental methods to evaluate factors influencing the heat gains for RDCs, the authors of the presented work adopted the Co-Heating method, which is used for the evaluation of the overall heat transfer coefficient of a building “as built” (Sonderegger and Modera, 1979). The methodology implies that a building is heated to an elevated indoor temperature ($T_{In} = T_{Amb} + \Delta T$) while the supplied heating power is monitored ($\dot{Q}_{Supply}$). The overall heat transfer coefficient ($K_{Building}$) is then found as: $K_{Building} = \dot{Q}_{Supply}/\Delta T$. In an ideal case, the measurements are conducted at stable indoor and ambient temperature conditions and without any external heat gains that influence the controlled supplied heating power that elevates the indoor temperature. However, in the case of buildings, the outdoor climate variations and intermittent solar heat gains pose a challenge to estimate the overall heat transfer coefficient accurately (Bauwens and Roels, 2014). If stable ambient conditions can be achieved, e.g. if the test object is located indoors, the precision of the Co-Heating method is substantially increased (Sasic Kalagasidis et al., 2016).

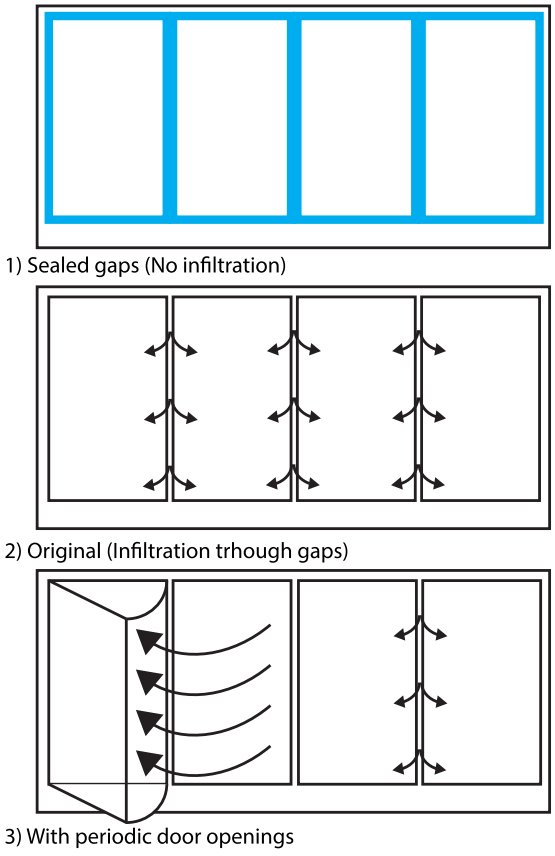

Fig. 2. Illustration of the test series used for the experiments. Test (1) with all gaps sealed. Test (2) with the RDC in its original setup. Test (3) with motors attached to induce dynamic door openings.

By applying this methodology to an RDC in an experimental series of three tests as described in Section 2, the K_{Env}, $\dot{m}_{Inf}$ and $m_{Opening}$ as well as the heat capacity C_{RDC} can be evaluated.

This study presents the novel application of the adapted Co-Heating method to an RDC equipped with four doors. In analogy with both the Tracer Gas article (Amin et al., 2009) and the Enthalpy method article (Navaz et al., 2005), the infiltration measurements from the Co-Heating experiments are validated towards the results of experiments conducted following the Condensate collection method. The Condensation collection method is, however, not explicitly defined in the available literature and is therefore fully described and derived in this article.

2. Method

The adapted Co-Heating method as described in Section 2.1 was applied to an empty RDC to evaluate its thermal performance in terms of heat transfer coefficient of the envelope (K_{Env}), heat capacity of the RDC (C_{RDC}), infiltration through gaps ($\dot{m}_{Inf}$) and infiltration caused by door openings ($m_{Opening}$). The Condensate collection method as described in Section 2.2 was then applied to the same RDC to validate the infiltration measurements.

Both methods were applied in a series of three test variations:

Test (1) – Doors closed and all gaps between the doors and the RDC sealed with tape.

Test (2) – Doors closed but gaps not sealed. (Original design)

Test (3) – Doors opened and closed periodically.

Fig. 2 illustrates the test variations. For Test (1), gaps around the doors were sealed with tape ensuring an airtight seal. All visible gaps of the RDC except the drain pipe were sealed. Internally

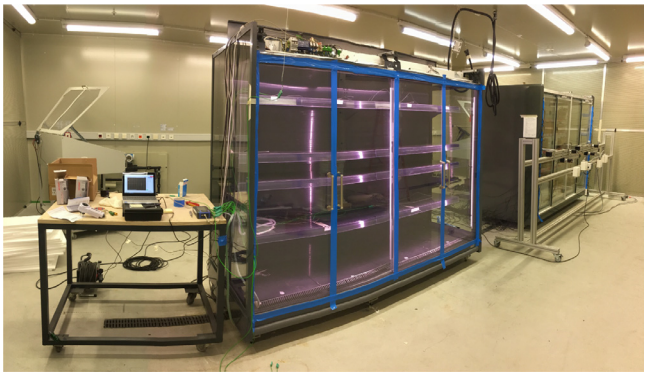

Fig. 3. Photo from the test room showing the RDC prepared for Test (1) with sealed gaps. Data logging equipment is located to the left of the RDC. The RDC located further to the right was inactive during all experiments.

the drain was covered with a fine grille, which was connected via a 90° elbow joint to a 2 m long pipe with a diameter of 50 mm. The infiltrating air through this pipework was considered to have a negligible contribution in comparison with the overall infiltration and was therefore left unsealed. Test (1) is primarily used for the evaluation of the heat transfer coefficient for the envelope, which in combination with Test (2) is required for the evaluation of the infiltration through gaps by the Co-Heating method. From Test (2), the infiltration rate through gaps is directly evaluated by the Condensation collection method. The infiltration caused by the door openings can be estimated by subtracting the estimated idle infiltration rate from the infiltration rate evaluated in Test (3).

Both Test (1) and Test (2) are conducted under stationary conditions. For the dynamic Test (3), each door was opened for 15 s every 66 s, i.e. 4 openings per 66s for the RDC $f_{Openings} = 0.0606$ Hz.

The RDC used in the experiment was a 2016 *KMW model FR4D-VSST-G* equipped with four double-glazed doors, placed in a temperature and humidity-controlled room complying to the demands of ISO 23953-2 (ISO, 2005). Fig. 3 shows a photo from the test room with the RDC prepared for Test (1) with sealed gaps.

2.1. Co-Heating method

This test is conducted by placing two electrical heating rods with a known power in the RDC while measuring the temperature development of the air in the RDC. Once a steady-state temperature is reached, the heat transfer coefficient can be evaluated, and the infiltration can be estimated. The transient regime of the heating process is used for the estimation of the heat capacity for the RDC. The refrigeration was de-activated during the full duration of the Co-Heating experiments.

The calculation of infiltration rate by the Co-Heating method is based on two balancing equations, namely the mass balance of air and the sensible heat balance. The two balances are shown in Fig. 4 and described in Eqs. (1) and (2).

$$\dot{m}_{Inf} - \dot{m}_{Exf} = 0 \tag{1}$$

$$\dot{Q}_{Supply} - \dot{Q}_{Env} + \dot{Q}_{Inf} - \dot{Q}_{Exf} = 0 \tag{2}$$

The difference in $\dot{Q}_{Inf} - \dot{Q}_{Exf}$ represents the heat flow caused by leakages in the envelope. Assuming no re-circulation of exfiltrated air, i.e. that ambient air is infiltrated and air from the gross volume is exfiltrated, the expression can be rewritten as:

$$\dot{Q}_{Inf} - \dot{Q}_{Exf} = \dot{m}_{Inf} c_p T_{Amb} - \dot{m}_{Exf} c_p T_{RDC} \tag{3}$$

Rearranging Eq. (1) gives that $\dot{m}_{Inf} = \dot{m}_{Exf}$, and by approximating the specific heat capacity of air, c_p, to be constant for the temperature range in the experiment, Eq. (4) can be derived.

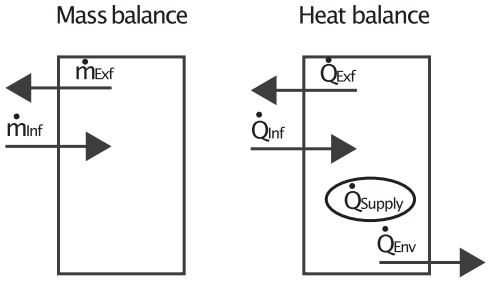

Fig. 4. Left: Mass balance of air within the fixed volume of the RDC where infiltration is balanced by exfiltration. Right: Heat balance of the RDC in its original setup where three unknown fluxes are contributing to the overall balance.

$$\dot{Q}_{Inf} - \dot{Q}_{Exf} = \dot{m}_{Inf} c_p (T_{Amb} - T_{RDC}) \tag{4}$$

Now inserting Eq. (4) into (2) gives Eq. (5) where $\dot{m}_{Inf}$ is the unknown variable and $\dot{Q}_{Env}$ can be quantified either by experiment as Test (1) or calculations.

$$\dot{Q}_{Supply} - \dot{Q}_{Env} + \dot{m}_{Inf} c_p (T_{Amb} - T_{RDC}) = 0 \tag{5}$$

By sealing the RDC as described in Test (1), the infiltration term disappears, and the heat transfer coefficient for the RDC envelope K_{Env} can be evaluated as shown in Eq. (6).

$$K_{Env} = \frac{\dot{Q}_{Supply}}{T_{RDC} - T_{Amb}} \tag{6}$$

$\dot{Q}_{Env}$ can be described as $K_{Env}(T_{RDC} - T_{Amb})$ and inserted to Eq. (5). By rearranging this expression, the infiltration rate, $\dot{m}_{Inf}$, can be written as a function of the measured quantities as shown in Eq. (7).

$$\dot{m}_{Inf} = \frac{\dot{Q}_{Supply} - K_{Env}(T_{RDC} - T_{Amb})}{c_p (T_{RDC} - T_{Amb})} \tag{7}$$

2.1.1. Heat capacity of an empty RDC

The heat capacity of the RDC can be estimated based on the data from the transient regime generated in the initialisation of Test (1). For an RDC that initially has the same internal temperature as the ambient, the transient RDC temperature development can be described as shown in Eq. (8), where $T_{RDC,\infty}$ is the balancing temperature for when a steady-state condition has been reached, i.e. the balancing temperature used for the evaluation of K_{Env} in Test (1).

$$T_{RDC}(t) = T_{RDC,\infty} + (T_{Amb} - T_{RDC,\infty}) e^{-t(K_{Env}/C_{RDC})} \tag{8}$$

The thermal inertia C_{RDC} is then evaluated based on a curve fit of Eq. (8) to the measured data. An example is given in Section 3.1.

2.1.2. Experimental setup

The temperature was recorded at a sample rate of $30s^{-1}$ with a *HIOKI LR8431* data logger connected to eight K-type thermocouples, positioned as shown in Fig. 5. Sensors 4 and 1 failed during the preparations of the experiment and were, therefore, excluded from the results and experimental setup. The setup was calibrated with an accuracy of ±0.1 °C prior to the execution of the experiment.

The internal heat gains, $\dot{Q}_{Supply}$, comprise of the circulation fans (137.2 W), internal lights (70.0 W) and a longitudinal heating rod (911.3 W) located in the front of the RDC as indicated in Fig. 5. The supplied electrical power was measured with a *Voltcraft EnergyLogger 4000*, with a 1% accuracy according to the manufacturer's specifications.

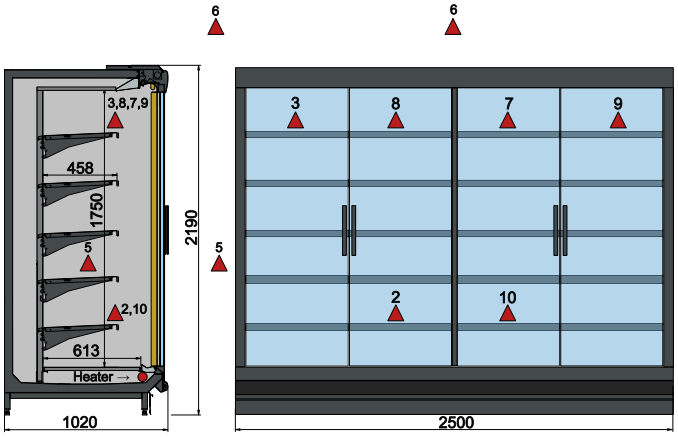

Fig. 5. Illustration of the sensors and heater placement in the RDC for the Co-Heating experiments. Sensors 5 and 6 are located in the ambient air in front of and besides the RDC respectively. Sensors 4 and 1 failed and were, therefore, excluded. *Left:* Section drawing. *Right:* Front view.

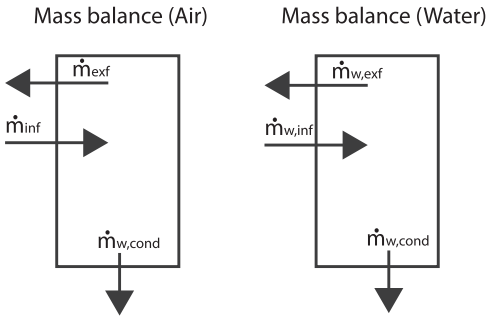

Fig. 6. Left: Mass balance of moist air and water within the fixed volume of the RDC. Right: Mass balance of water vapour and liquid in the RDC.

2.2. Condensate collection method

This test is conducted by monitoring the temperature and humidity of the ambient air and the air in the RDC, as well as the mass of the condensed water. During the full duration of the Condensation collection experiments, the refrigeration was activated for the RDC. The temperature set-point was adjusted so that the evaporator temperature was kept above the freezing point of water to ensure that no accumulation of frost occurred on the evaporator.

The evaluation of infiltration rate by the Condensate collection method is based on the mass balance of moist air and the mass balance of water as shown in Eqs. (9) and (10) and depicted in Fig. 6.

$$\dot{m}_{Inf} - \dot{m}_{Exf} - \dot{m}_{W,Cond} = 0 \tag{9}$$

$$\dot{m}_{W,Inf} - \dot{m}_{W,Exf} - \dot{m}_{W,Cond} = 0 \tag{10}$$

These formulations can be expressed as Eqs. (11) and (12) where the water vapour mass in the air is defined by the moisture ratio X_i g/g_D. These formulations are valid if no re-circulation of exfiltrating air is present, i.e. ambient air is infiltrating and air from the gross volume of the RDC is exfiltrating.

$$(1 + X_{Amb})\dot{m}_{D,Inf} - (1 + X_{RDC})\dot{m}_{D,Exf} - \dot{m}_{W,Cond} = 0 \tag{11}$$

$$X_{Amb}\dot{m}_{D,Inf} - X_{RDC}\dot{m}_{D,Exf} - \dot{m}_{W,Cond} = 0 \tag{12}$$

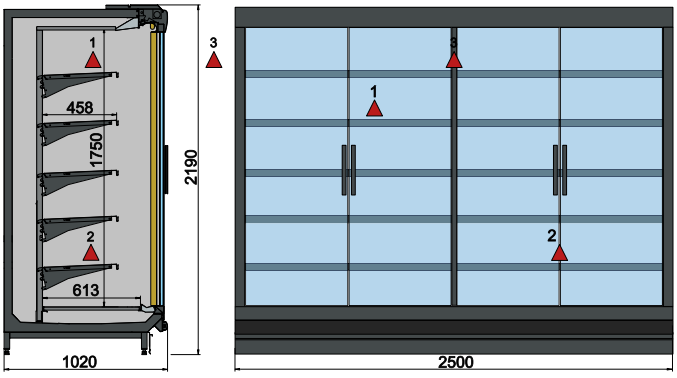

Fig. 7. Illustration of sensor placement in the RDC for the Condensation collection experiments. Sensor 3 is located in the ambient in front of the RDC. *Left:* Section drawing. Right: *Front* view.

By isolation of $\dot{m}_{D,Exf}$ in Eq. (11), this expression can be inserted to Eq. (12), where $\dot{m}_{D,Inf}$ is isolated as shown in Eq. (13).

$$\dot{m}_{D,Inf} = \frac{\dot{m}_{W,Cond}}{X_{Amb} - X_{RDC}} \tag{13}$$

Eq. (13) expresses the mass flow rate of dry air into the RDC as a function of the condensate flow and ambient moisture ratio. Hence, the mass flow rate of the infiltrating air can be expressed as shown in Eq. (14).

$$\dot{m}_{Inf} = \frac{(1 + X_{Amb})\dot{m}_{W,Cond}}{X_{Amb} - X_{RDC}} \tag{14}$$

2.2.1. Experimental setup

The temperature and RH were recorded at a sample rate of 30 s^{-1} by three separate loggers [*Clas Ohlsson ST-171*] with an absolute accuracy of $\pm$ 3% for RH and $\pm$0.5 °C fort temperature. Individual differences between the loggers were controlled prior to the experiment and were found to be $<$ 1% for RH and $<$ 0.2 °C for temperature. Two loggers were placed in the RDC and one logger in the test room as illustrated in Fig. 7.

The condensed water was collected in a container connected to the drainpipe of the RDC. The mass of the container was measured hourly ($\pm$60 s) with an accuracy of $\pm$1 g.

2.3. Infiltration per opening

Both methods evaluate the average infiltration rate of $\dot{m}_{Inf}$ in kg/s over the time period of the experiment. As shown in Eq. (15), the influence of door openings can be evaluated by subtracting the results from the dynamic Test (3) from the idle infiltration rate from Test (2).

$$\dot{m}_{Inf,3} - \dot{m}_{Inf,2} = \dot{m}_{Openings} \tag{15}$$

The infiltration caused by each door opening can be obtained as described in Eq. (16).

$$\frac{\dot{m}_{Openings}}{f_{Openings}} = m_{Opening} \tag{16}$$

2.4. Properties of moist air

To evaluate the infiltration for the Condensation collection method, the measured *RH* is translated to moisture ratio (X_i g/g_D), which can be expressed as a function of the partial pressure as shown in Eq. (17) (ASHRAE, 2017).

$$X_i = \frac{0.621945\, p_{Ws} \cdot RH}{p_T - p_{Ws}} \tag{17}$$

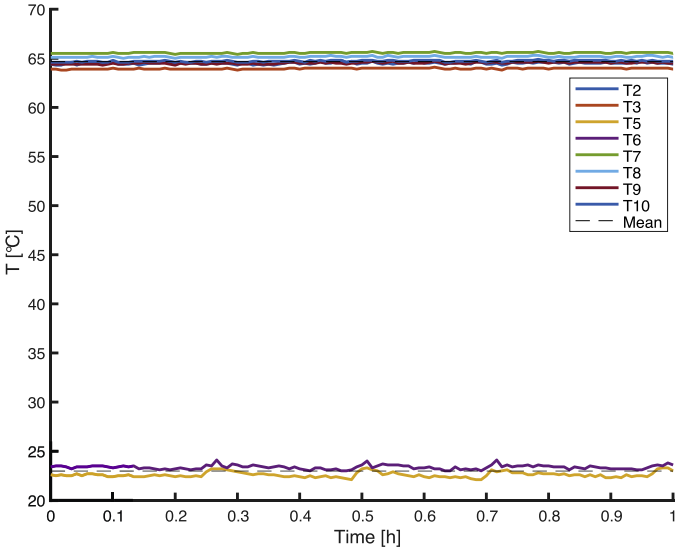

Fig. 8. Temperature data for 1 h from the Co-Heating Test (1) with all gaps sealed. Average temperature over time for $T_{RDC} = 64.66$ °C and $T_{Amb} = 22.98$ °C as indicated by the dashed lines.

The total pressure (p_t) is considered to be constant at 101 325 Pa during the experiment. The saturated vapour pressure p_{Ws} was found from interpolation between tabulated values in ASHRAE (2017).

In the Co-Heating method, the thermal heat capacity of air is assumed to be $c_{p,Air} = 1006$ J/kg · K (ASHRAE, 2017).

The temperature- and moisture-dependent density is estimated as described by Eq. (18), where the universal gas constant for dry air is $R_D = 287.058$ J/kgK and for water vapour $R_W = 461.495$ J/kgK (ASHRAE, 2017).

$$\rho_{Air} = \frac{p_0 - (RH \cdot p_{Ws})}{R_D \tau} + \frac{RH \cdot p_{Ws}}{R_W \tau} \tag{18}$$

3. Results and discussion

The results for each testing method are first presented separately, followed by a comparison between evaluated quantities and methods.

3.1. Co-Heating

For Test (1), the RDC was heated to 64.66 °C by a constant supply of 1118.5 W consisting of the summed electrical power from the heater, fans and lights within the RDC gross volume. In Fig. 8, the temperature data used for the evaluation of K_{Env} are illustrated in a line graph. During Test (1), all visible gaps were sealed. However, any infiltration caused by imperfections or through the drain would be included in the overall heat transfer coefficient K_{Env}. From the results, it could be concluded that the heat transfer coefficient of the RDC envelope $K_{Env} = 26.83$ W/K.

Additionally from Test (1), the thermal inertia (C_{RDC}) of the RDC was evaluated by performing a geometric curve fit of Eq. (8) on the measured data as shown in Fig. 9. The best fit was found for $C_{RDC} = 283$ kJ/K. The red lines show the sensitivity band for the estimation of C_{RDC} where the fitted value was increased and decreased by ± 10%. As shown, the curve is not following the temperature increase during the first hour of the experiment. This is a consequence of a delayed start of the heaters while the temperature increased due to the heat gains from the fans and lights. This period has been neglected since it has a negligible impact on the evaluated value for C_{RDC}.

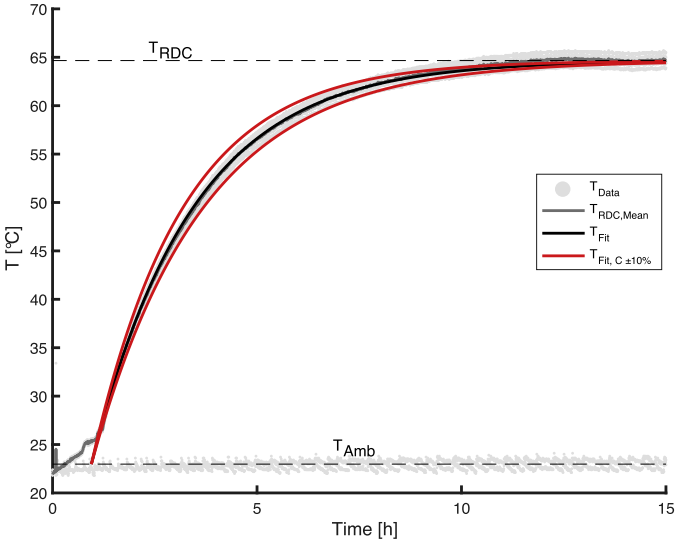

Fig. 9. Transient temperature development for the RDC when Co-Heating Test (1) was initiated. All temperature data-points indicated with light-grey dots. A geometric curve fit of Eq. (8) is illustrated by the black line. The red lines show the impact of increasing or decreasing the value of C_{RDC} by ± 10%. (For interpretation of the references to color in this figure legend, the reader is referred to the web version of this article.)

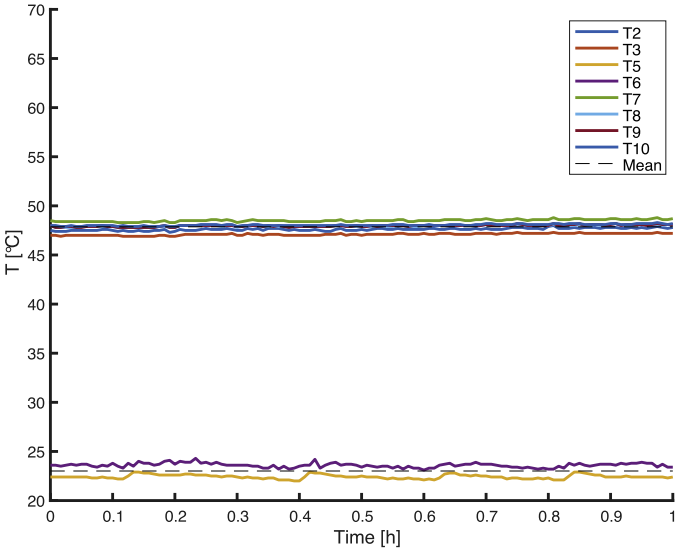

Fig. 10. Temperature data for 1 h from the Co-Heating Test (2) with no gaps sealed on the RDC. $T_{RDC} = 47.87$ °C and $T_{Amb} = 23.01$ °C as indicated by the dashed lines.

For Co-Heating Test (2), the tape seal was removed, and the RDC was left idle with the heater, lights and fans active until a new and lower equilibrium temperature inside the RDC was reached. Fig. 10 illustrates the decreased T_{RDC} and constant T_{Amb}, indicating that infiltration through the gaps significantly affected the overall heat transfer coefficient of the RDC. By inserting the measured temperatures (T_{Amb} T_{RDC}) into Eq. (7), it was found that the idle infiltration through gaps was $\dot{m}_{Inf,COH2} = 0.0181$ kg/s. Alternatively, in terms of equivalent heat transfer coefficient based on Eq. (6), $K_{COH2} = 45.00$ W/K i.e. 67 % higher than with sealed gaps.

For Co-Heating Test (3), the doors were opened individually every 66 s. Hence, the temperature of the RDC, T_{RDC}, decreased further and got stabilised at 34.48 °C as shown in Fig. 11. The thermal inertia of the RDC smooths periodic variations in temperature that the RDC door openings cause, allowing to reach a quasi-steady

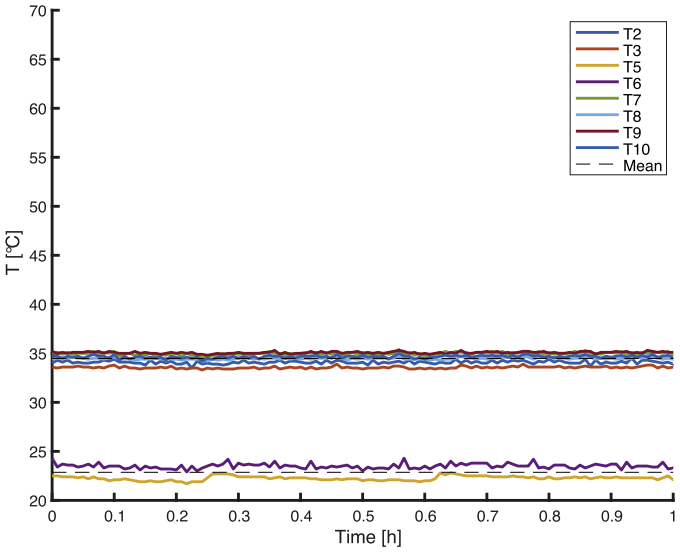

Fig. 11. Temperature data for 1 h from the Co-Heating Test (3) where the doors were opened periodically. $T_{RDC} = 34.48$ °C and $T_{Amb} = 22.86$ °C as indicated by the dashed lines.

Table 1
Overview of measured data and conditions during the Co-Heating experiments.

	Test 1	Test 2	Test 3	Unit
T_{Amb}	22.98	23.01	22.86	°C
ρ_{Amb}	1.18	1.18	1.18	kg/m^3
T_{RDC}	64.66	47.87	34.48	°C
ρ_{RDC}	1.04	1.09	1.14	kg/m^3
$\dot{Q}_{Supply}$	1 118.5	1 118.5	1 118.5	W

state. Based on Eq. (7), the infiltration rate during this opening scenario was $\dot{m}_{Inf,\mathrm{COH3}} = 0.0691$ kg/s.

Furthermore, based on Eq. (16) the infiltrating mass per door opening can be evaluated as, $m_{opening,\mathrm{COH}} = 0.8800$ kg at the specific conditions.

Table 1 shows the measured quantities from all three experiments.

3.2. Condensate collection

By sealing the RDC and applying Test (1), the Condensation collection method should result in *nil* condensate flow for a sealed RDC. However, from Test (1) it was seen that a mass flow of condensate water $\dot{m}_{Cond,1} = 4.5 \cdot 10^{-}6$ kg/s was present when measured 60 h after the seal was applied. This indicates an unintended infiltration of $\dot{m}_{Inf,\mathrm{CO1}} = 0.00067$ kg/s due to imperfections in the envelope or sealing tape and through the drainpipe. This amount is negligible and it is included in the total infiltration measured in Test (2).

The temperature of the evaporator varied during the test period due to the chosen temperature control strategy of the RDC. Hence, as shown in Fig. 12, the de-humidification varied in time, which is reflected in the fluctuating moisture ratio. Thus, a quasi-steady state was reached by averaging the data over a 4-h time frame. For the calculation of the infiltration rate in Test (2), the mean measured moisture ratio from Fig. 12 and the measured condensate flow of $\dot{m}_{\mathrm{CO2}} = 1.54 \cdot 10^{-4}$ kg/s are used, resulting in an estimation of the infiltration through gaps to be $\dot{m}_{Inf,\mathrm{CO2}} = 0.0234$ kg/s.

For Test (3), the doors were periodically opened, causing a significant increase in heat extraction demand due to the infiltrating air. Consequently, a more stable evaporator temperature was

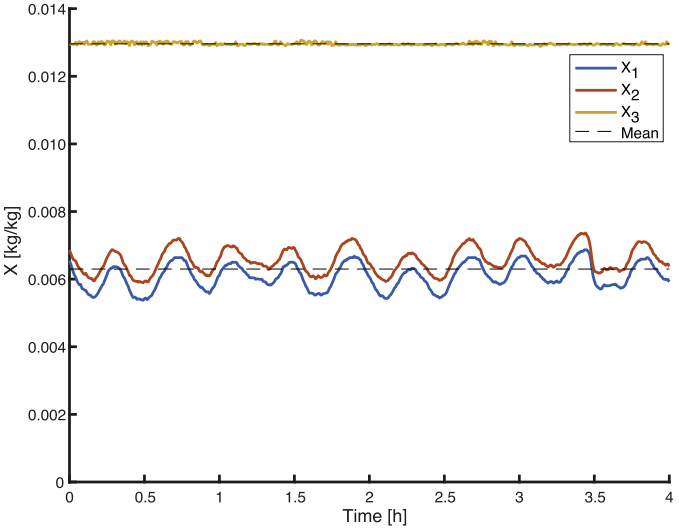

Fig. 12. Moisture ratio data for 4 h from the Condensate collection Test (2) with no gaps sealed on the RDC. $X_{RDC} = 0.0063$ g/g$_D$ and $X_{Amb} = 0.0130$ g/g$_D$ as indicated by the dashed lines.

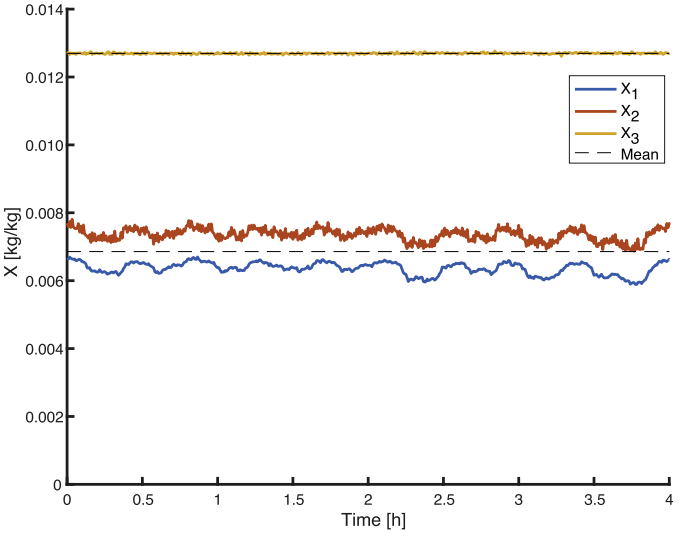

Fig. 13. Moisture ratio data for 4 h from the Condensate collection Test (3) where the doors were opened periodically. $X_{RDC} = 0.0069$ g/g$_D$ and $X_{Amb} = 0.0127$ g/g$_D$ as indicated by the dashed lines.

Table 2
Overview of measured data and conditions during the Condensation collection experiments.

	Test 1	Test 2	Test 3	Unit
T_{Amb}	26	25.92	25.70	°C
X_{Amb}	0.0126	0.0130	0.0127	g/g$_D$
ρ_{Amb}	1.17	1.17	1.17	kg/m^3
T_{RDC}	7.5	7.80	9.58	°C
X_{RDC}	0.0058	0.0063	0.0069	g/g$_D$
ρ_{RDC}	1.25	1.25	1.24	kg/m^3
$\dot{m}_{W,Cond}$	$4.5 \cdot 10^{-6}$	$1.54 \cdot 10^{-4}$	$4.49 \cdot 10^{-4}$	kg/s

achieved, leading to decreased fluctuations in moisture ratio, as shown in Fig. 13. From the results, an infiltration of $\dot{m}_{Inf,\mathrm{CO3}} = 0.0779$ kg/s was found. By subtracting $\dot{m}_{\mathrm{CO2}}$ from $\dot{m}_{\mathrm{CO3}}$, the influence of the door openings was estimated. Furthermore, based on Eq. (16), the difference could be translated to an infiltrating mass per door opening, $m_{opening,CO} = 0.9407$ kg.

Table 3
Overview of the calculated results from the Co-Heating and Condensation collection experiments for infiltration and thermal performance.

	Test 1	Test 2	Test 3	Unit
Co-Heating				
K_i	26.83	45.00	99.31	W/K
C_{RDC}	283			kJ/K
$\dot{m}_{Inf}$	–	0.0181	0.0691	kg/s
$m_{Opening}$			0.8800	kg
Condensation				
$\dot{m}_{Inf}$	0.00067	0.0234	0.0779	kg/s
$m_{Opening}$			0.9407	kg

Table 4
Corresponding initial infiltration rate and correction factor ξ_i based on the specific conditions at each Test.

	Test 1	Test 2	Test 3	Unit
Co-Heating				
ξ_i	–	0.9237	0.9661	–
$\dot{m}_{Inf,Corr}$	–	0.0195	0.0715	kg/s
$m_{Opening,Corr}$			0.8961	kg
Condensation				
ξ_i	1.0684	1.0684	1.0598	–
$\dot{m}_{Inf,Corr}$	–	0.0219	0.0735	kg/s
$m_{Opening,Corr}$			0.8906	kg

Table 2 shows the measured quantities and test room conditions.

3.3. Comparison of results

In Table 3, the results from each test and method are tabulated for easy reference.

For Test (1) with the sealed RDC, the Condensation collection method indicates that the RDC is not perfectly sealed. The infiltrating mass flow was $\dot{m}_{CO,1} = 0.00067$ kg/s. For the Co-Heating method, such imperfections cannot explicitly be seen as the method is based on the heat balance of the RDC, which assumes no infiltration. Thus, the effects of imperfections are included in the heat transfer coefficient of the envelope.

From Test (2), the Condensation method indicates a 0.0053 kg/s (23%) higher infiltration rate than the Co-Heating method. A marginal part of the discrepancy can be explained by infiltration through imperfections ($\dot{m}_{CO,1}$). However, the expansion or contraction of the infiltrating air parcel due to changes in density has a significantly stronger influence. For the Condensation collection method, the infiltrating parcel of ambient air contracts once its temperature is lowered in the RDC. Hence, additional ambient air infiltrates to the RDC to equalise the pressure difference between the fixed volume of the RDC and the ambient. This process starts with an initial volume infiltrating and repeats for parcels with decreasing volume until the pressures are at equilibrium. The ratio between the initial infiltrating parcel and the measured total infiltrated volume of the thermal expansion/contraction is described in Eq. (19).

$$\xi_i = \sum_{n=1}^{\infty} (1 - \rho_{Amb}/\rho_{RDC})^{(n-1)} \tag{19}$$

As shown in Eq. (20), the mass of the initially infiltrated parcel can be determined by dividing the measured infiltration by the factor ξ_i. Additionally, the factor allows adjustment of the measured infiltration at higher temperatures in the Co-Heating experiment to conditions for RDCs in operation.

$$\dot{m}_{i,Corr} = \frac{\dot{m}_i}{\xi_i} \quad \Leftrightarrow \quad \dot{m}_i = \dot{m}_{i,Corr} \cdot \xi_i \tag{20}$$

Table 4 shows the corresponding initial infiltration. As shown, the discrepancies has significantly decreased. Hence, the results are converging with an accuracy well within the error range of the measurements.

The results can be adjusted to an equivalent infiltration occurring at the same conditions as the Condensation collection experiment by applying the correction factor $\xi_{Test\ 2} = 1.0684$ to the initial infiltration from the Co-Heating experiment. The adjusted equivalent infiltration from Test (2) was found to be 0.0208 kg/s compared with 0.0234 kg/s from the Condensation collection experiment. In analogy, the mass of infiltrating air per door opening from Co-Heating experiment was found to be 0.9497 kg compared with 0.9407 kg for the Condensate collection method.

4. Comparison of methods for the evaluation of infiltration

The Condensation collection method, Entalphy method and Tracer gas method were briefly described in the introduction of this article. All three methods are solely focused on the evaluation of the infiltration to the RDC. Both the Condensation collection method and the Tracer gas method could be applied to a closed RDC for the evaluation of infiltration through gaps and caused by door operations. The Enthalpy method does however require a measuring point in the spilling air from the air curtain of the RDC, which for an open RDC would be uniform in the longitudinal direction of the RDC. For a closed RDC, this effect would vary due to the influence of intermittent vertical gaps causing local variations of air-flow, temperature and moisture content. Therefore, the methodology cannot be applied to a closed RDC without modifications. In Table 5, the Condensation collection, Enthalpy and Tracer gas methods are compared with the adapted Co-Heating method.

When comparing the infiltration rates through gaps, Test (2), as evaluated by the Co-Heating test to the Condensation collection method, it was found to be 11% lower and only 3% lower for Test (3) with dynamic door operations. The error caused by the precision of the instruments is less than 2% for both methods, meaning that the discrepancies must be caused by other factors. As it can be seen in the presented data from the experiments, the temperature within the RDC varies with 2 °C and the moisture ratio varies with 0.0015 g/g_D, causing uncertainties for the measurements due to spatial variations. For the Co-Heating test, the internal average temperatures of the RDC were estimated based on six measuring points, lowering the impact of local discrepancies. For the condensate collection method, there were only two measuring points in the RDC and the uncertainties are therefore more significant. This could be mitigated in future applications by the introduction of more measurement points in the RDC.

For the Tracer gas method and Enthalpy method, the locations of the measurements are specific regions within or around the RDC. This implies that the methods are sensitive to non-uniform fields. For the measurement in the return air, the temperature is known to be non-uniform (Månsson, 2016) with a temperature gradient up to 4 °C per 5 mm perpendicular from the floor. Hence there is a need for several distributed measuring points within each region to ensure an accurate average. Besides the uncertainties caused by the locations of the measurements, both the Tracer gas and Enthalpy methods are based on the mass flow rate of the fan in the RDC, which is challenging to measure with a high accuracy.

Other important aspects for the methods are the associated cost, time and effort it takes to execute the experiments. The Tracer gas test can generate results already after 15 min (Amin et al., 2009) as the stable equilibrium concentration of the trace gas is reached very fast. The other presented methodologies need to initialise longer to ensure a steady state temperature and/or moisture content in the RDC. It is, however, possible to setup the measuring equipment while the RDC is running, i.e.

Table 5
Comparison matrix of methods for evaluating the thermal performance and infiltration of an RDC.

	Condensation (Faramarzi, 1999)	Enthalpy (Navaz et al., 2005)	**Tracer gas** (Amin et al., 2009)	Co-Heating –
Time	15+4 h(1 h[a])	15+4 h(1 h[a])	15 min	15 h+1 h (15 min[a])
Equipment	2 × RH+T Logger 1 × Scale	4 × RH+T Logger 1 × Air Flow meter	Gas injection system Gas sampling system Tracer gas 2 × T Logger 1 × Air Flow meter	1 × Heater 2 × T Logger
Min. cost[b]	$200	$900	$3000	$200
RDC type	Open/Closed	Open	Open/Closed	Open/Closed
Active refrigeration	Yes	Yes	No/Yes	No
Ambient conditions	High Steady RH	Steady T&RH	Steady T	Steady T
Evaluated variables				
K_{Env}	–	–	–	✓
C_{RDC}	–	–	–	✓
$\dot{m}_{Inf.Idle}$	✓	✓	✓	✓
$m_{Opening,Door}$	✓	–	✓	✓
Comments				
	Drainpipe must be connected to reservoir. Ambient dew-point higher than T_{RDC}.	Mass-flow of circulating air must be known to quantify $\dot{m}_{Inf}$.	Corr. factor needed if no refrigeration is present.	Corr. factor needed due to high temperatures, i.e. density change.

[a] At steady state conditions.
[b] Excluding costs of door opening automation and other infrastructure components.

the setup time can be included in the initialisation time. For the Tracer gas method, the equipment must be installed prior to the test, adding the needed time of installation to the startup time.

The tracer gas equipment consists of a gas injection system ensuring that the gas is distributed uniformly. Additionally, a gas analyser connected to a gas sampling system is required to measure the concentration in the locations defined in the method. Moreover, the massflow rate of the discharge air in the RDC must be measured. In general terms, the setup is rather complex and consists of delicate equipment that requires a minimum budget of $3000 to perform a test.

The Co-Heating and the Condensation collection methods are on the other hand both based on simpler equipment and can be executed with an equipment budget as low as $200. These methods are also independent of the air discharge mass flow rate, which increase the accuracy of the evaluated infiltration rate.

5. Conclusions

The aim of the presented study was to develop a simple experimental methodology for the evaluation of the thermal performance of RDCs. The results for both infiltration through gaps at idle state and the infiltration caused by door openings show good conformity when comparing the values from the Co-Heating method with the results from the Condensate collection method. In addition to the results on infiltration, the Co-Heating method evaluates the heat transfer coefficient K_{Env} and the heat capacity C_{RDC} of the RDC. Hence, the adapted Co-Heating method presented in this article assembles a complete methodology for evaluating the necessary variables for the evaluation of the infiltration and thermal performance of an RDC.

The methodology can be applied to RDCs at any location where the ambient temperature is constant, i.e. the existing stock of RDCs within a supermarket can conveniently be assessed. It does, however, demand that the tested RDC temperature is increased beyond ambient temperature, which might damage the stored food unless removed.

As a complementary for the evaluation of infiltration only, the condensation collection method can be applied in an operational supermarket without interfering with the stock of refrigerated foods.

From the results it was found that the infiltration for the tested RDC with four doors is approximately 0.022 kg/s and that one door opening with a duration of 15 s would cause approximately 0.94 kg of ambient air to infiltrate to the RDC.

Declaration of Competing Interest

The authors declare that they do not have any financial or non-financial conflict of interests

Acknowledgments

The authors would like to thank the main funding body, EIT Climate-KIC, that provided not just the necessary funds but also an invaluable network and inspirational community. Also, the authors would like extend their special thanks to KMW Kühlmöbelwerk Limburg GmbH for generously sharing their test facilities and expertise.

References

Albayati, I.M., Postnikov, A., Pearson, S., Bickerton, R., Zolotas, A., Bingham, C., 2020. Power and energy analysis for a commercial retail refrigeration system responding to a static demand side response. Int. J. Electr. Power Energy Syst. 117 (December 2019), 105645. doi:10.1016/j.ijepes.2019.105645.
Amin, M., Dabiri, D., Navaz, H.K., 2009. Tracer gas technique: a new approach for steady state infiltration rate measurement of open refrigerated display cases. J. Food Eng. 92 (2), 172–181. doi:10.1016/j.jfoodeng.2008.10.039.
ASHRAE, 2017. In: ASHRAE (Ed.), 2017 ASHRAE Handbook – Fundamentals (SI-Edition), 2017. ASHRAE, Atlanta.
Bauwens, G., Roels, S., 2014. Co-heating test: a state-of-the-art. Energy Build. 82, 163–172. doi:10.1016/j.enbuild.2014.04.039.
Faramarzi, R., 1999. Efficient display case refrigeration. ASHRAE J. 41 (11), 46–54.
Faramarzi, R.T., Coburn, B.A., Sarhadian, R., 2002. Performance and energy impact of installing glass doors on an open vertical deli/dairy display case. ASHRAE Trans. 108 PART 1, 673–679.
Farhangi, H., 2010. The path of the smart grid. IEEE Power Energy Mag. 8 (1), 18–28. doi:10.1109/MPE.2009.934876.
Funder, T., 2015. Supermarkets as an important smart grid application. In: Proceedings of the 16th European Conference, Technological Innovations in Refrigeration And in Air Conditioning. Danfoss, Milan, pp. 1–4.
Hovgaard, T.G., Halvgaard, R., Larsen, L.F.S., Jrgensen, J.B., 2011. Energy efficient refrigeration and flexible power consumption in a smart grid. In: Proceedings of Risø International Energy Conference, pp. 164–175.

ISO, 2005. EN ISO 23953-2:2005.
Khan, A.S.M., Verzijlbergh, R.A., Sakinci, O.C., De Vries, L.J., 2018. How do demand response and electrical energy storage affect (the need for) a capacity market? Appl. Energy 214 (July 2017), 39–62. doi:10.1016/j.apenergy.2018.01.057.
Månsson, T., 2016. Energy in Supermarkets. Chalmers University of Technology Licentiate thesis.
Månsson, T., Ostermeyer, Y., 2013. The potential of thermal energy storage in food cooling processes in retail markets for grid balancing. In: Proceedings of the Nordic Symposium on Building Physics 2013, pp. 1–6. Lund
Månsson, T., Ostermeyer, Y., 2019. Potential of Supermarket Refrigeration Systems for Grid Balancing by Demand Response. In: Proceedings of the 8th International Conference on Smart Cities and Green ICT Systems, pp. 1–6. Heraklion
Månsson, T., Rukundo, A., Almgren, M., Tsigas, P., Marx, C., Ostermeyer, Y., 2019. Analysis of door openings of refrigerated display cabinets in an operational supermarket. J. Build. Eng. 26, 100899. doi:10.1016/j.jobe.2019.100899.
Navaz, H.K., Henderson, B.S., Faramarzi, R., Pourmovahed, A., Taugwalder, F., 2005. Jet entrainment rate in air curtain of open refrigerated display cases. Int. J. Refrig. 28 (2), 267–275. doi:10.1016/j.ijrefrig.2004.08.002.
Orlandi, M., Visconti, F.M., Zampini, S., 2013. CFD assisted design of closed display cabinets. In: Proceedings of the 2nd IIR International Conference on Sustainability and the Cold Chain. International Institute of Refrigeration, Paris, pp. 1–8.
Pedersen, R., Schwensen, J., Biegel, B., Stoustrup, J., Green, T., 2014. Aggregation and control of supermarket refrigeration systems in a smart grid. IFAC Proc. Vol. (IFAC-PapersOnline) 19, 9942–9949. doi:10.3182/20140824-6-ZA-1003.00268.
Sasic Kalagasidis, A., Brycke, E., Nilssen, J., Johansson, P., 2016. Evaluation of a modified co-heating test for in-situ measurements of thermal transmittance of single-family houses. In: Proceedings of the 2016 Thermal Performance of the Exterior Envelopes of Whole Buildings, pp. 598–608. 2016-Decem
Sonderegger, R., Modera, M., 1979. Electric Co-Heating a method for evaluating seasonal heating efficiencies and heat loss rates in dwellings. In: Proceedings of the ASHRAE Semiannual Meeting, LA 1980, pp. 1–23. Copenhagen